MAGNETOHYDRODYNAMIC COMBUSTION

R. V. POLOVIN and V. P. DEMUTSKII

Physico-Technical Institute, Academy of Sciences, Ukr. S. S. R.

Submitted to JETP editor December 31, 1960

J. Exptl. Theoret. Phys. (U.S.S.R.) 40, 1746-1754 (June, 1961)

Possible combustion modes in a magnetohydrodynamic medium are determined. The types of magnetohydrodynamic shock and self-similar waves which can accompany magnetohydrodynamic combustion waves in the presence of a moving perfectly conducting piston are investigated. The piston velocity, the Alfvén velocity and the reaction energy are assumed to be sufficiently small. The conductivity of the medium is assumed to be infinite.

1. In recent years there has been an increased interest in new combustion modes. A number of papers is devoted to the problem of the combustion of fuel in a supersonic stream. In other papers, for example references 1 — 4, the effect of a magnetic field on detonation is investigated. In the present paper we investigate the effect of a magnetic field on the combustion process.

In ordinary hydrodynamics (in the absence of a magnetic field) two combustion modes are possible:

a) subsonic combustion

$$v_1 < c_1, \qquad v_2 < c_2; \tag{1}$$

b) supersonic combustion

$$v_1 > c_1, \qquad v_2 > c_2. \tag{2}$$

Here v is the velocity of the medium with respect to the discontinuity, c is the velocity of sound; subscript 1 refers to the region in front of the discontinuity and subscript 2 refers to the region behind the discontinuity.

If heating of the medium in front of the combustion wave occurs as a result of ordinary thermal conductivity then $v_1 \ll c_1$, and, therefore, supersonic combustion is usually impossible. Supersonic combustion can occur in the case of thermonuclear reactions when heating of the medium takes place by means of heat transfer by radiation; the supersonic combustion regime is also realized in the case of combustion in a supersonic stream.[5]

The difference between subsonic and supersonic combustion consists of the fact that in subsonic combustion the density is diminishing, while in supersonic combustion it is increasing.

In magnetohydrodynamics there exist three velocities of propagation of small disturbances: the Alfvén velocity $\mathbf{U} = \mathbf{H}/(4\pi\rho)^{1/2}$ and the velocities of propagation of the fast and the slow magnetoacoustic waves

$$U_\pm = \{U^2 + c^2 \pm [(U^2 + c^2)^2 - 4c^2 U_x^2]^{1/2}\}^{1/2}/\sqrt{2}$$

(the plus sign refers to the fast wave, and the minus sign refers to the slow wave, U_x is the component of the Alfvén velocity parallel to the direction of propagation of the wave). The existence of three characteristic velocities leads, as we shall see later, to the appearance of four magnetohydrodynamic combustion modes:

a) "slow" combustion

$$v_{1x} < U_{1-}, \qquad v_{2x} < U_{2-}; \tag{3}$$

b) "sub-Alfvén" combustion

$$U_{1-} < v_{1x} < U_{1x}, \qquad U_{2-} < v_{2x} < U_{2x}; \tag{4}$$

c) "super-Alfvén" combustion

$$U_{1x} < v_{1x} < U_{1+} \qquad U_{2x} < v_{2x} < U_{2+}; \tag{5}$$

d) "fast" combustion

$$U_{1+} < v_{1x}, \qquad U_x < v_{2x}. \tag{6}$$

(The subscript 1 refers to the region in front of the discontinuity, and the subscript 2 to the region behind the discontinuity; we recall that $U_- \leq U_x \leq U_+$.)

The difference between the four magnetohydrodynamic combustion modes lies not only in the different manner of density variation, but also in the different nature of variation of the magnetic field. As we shall show later, in the case of the slow and the super-Alfvén combustion the density is decreasing, while in the case of the sub-Alfvén and the fast combustion it is increasing. The magnetic field increases in the case of fast and slow combustion, and decreases in the case of the sub-Alfvén and the super-Alfvén combustion.

In magnetohydrodynamics, if the condition $U_1 \ll c_1$ is satisfied, slow, sub-Alfvén and super-Alfvén combustion can occur at temperatures common in the case of chemical reactions, and fast combustion can occur at thermonuclear temperatures.

Condensation discontinuities and photoionization discontinuities belong to the same type of discontinuities as combustion waves. Photoionization discontinuities occur in neutral interstellar gas in the case of intense radiation from a star (cf. references 6 — 8). The excess of photon energy over the ionization energy is released in the form of heat energy q. The velocity of propagation of a photoionization discontinuity can be both smaller than and greater than the velocity of sound.

2. At the surface of discontinuity the laws of conservation of mass, momentum and energy hold, and also the values of the tangential electric and of the normal magnetic field remain continuous:

$$\{(v_x - \zeta)/V\} = 0, \tag{7}$$

$$\{p + (v_x - \zeta)^2/V + H_y^2/8\pi\} = 0, \tag{8}$$

$$\{\gamma pV/(\gamma - 1) + (v_x - \zeta)^2/2 + v_y^2/2 + VH_y^2/4\pi - VH_xH_yv_y/4\pi\,(v_x - \zeta)\} = q, \tag{9}$$

$$\{(v_x - \zeta)\,v_y/V - H_xH_y/4\pi\} = 0, \tag{10}$$

$$\{H_xv_y - (v_x - \zeta)\,H_y\} = 0, \tag{11}$$

$$\{H_x\} = 0, \tag{12}$$

where $V \equiv 1/\rho$ is the specific volume, v is the velocity of the medium, ζ is the velocity of propagation of the combustion wave in the laboratory system of coordinates, p is the pressure, γ is the index of the Poisson adiabat which we assume for the sake of simplicity to be the same on both sides of the discontinuity, q is the energy released at the surface of discontinuity ($q > 0$); the x axis is directed normal to the discontinuity, and the system of coordinates is chosen in such a way as to make $H_z \equiv 0$ and $v_z \equiv 0$.

The conservation laws (7) — (12) are insufficient to determine the combustion mode uniquely. In order for combustion actually to take place it is necessary that in addition the evolutionary conditions should also be satisfied.[9-11] They consist of the requirement that the number of divergent waves on both sides of the surface of discontinuity should be equal to the number of independent boundary conditions.

Unlike shock waves and overcompressed detonation waves, the speed of propagation of a combustion wave in a medium at rest does not depend on the amplitude of the wave, but is determined by the physico-chemical characteristics of the medium in front of the wave.[12] Therefore, when a combustion wave is perturbed the velocity of propagation of the wave remains constant. This leads to the result that in order for the evolutionary conditions to be satisfied in ordinary hydrodynamics (in the absence of a magnetic field) the number of diverging waves must be equal to three, while in magnetohydrodynamics the number of diverging waves must be equal to seven. From this it follows that only such combustion waves are possible for which the inequalities (1), (2), and (3) — (6) are satisfied. The evolutionary conditions (3) — (6) restrict the number of waves which can be simultaneously propagated in one direction.

In the case of fast combustion the combustion wave can be followed by a fast magnetoacoustic (shock or self-similar) wave, and this can be followed by an Alfvén discontinuity, and, finally, by a slow (shock or self-similar) wave. Not a single one of the magnetohydrodynamic waves can be propagated ahead of the fast combustion wave.

In the case of super-Alfvén combustion the fast (shock or self-similar) wave leads, followed by a super-Alfvén combustion wave, then by an Alfvén discontinuity and, finally, by a slow wave.

In the case of sub-Alfvén combustion the fast wave leads, followed by the Alfvén discontinuity, then by a sub-Alfvén combustion wave and, finally, by a slow wave.

In the case of slow combustion the fast wave leads, followed by the Alfvén discontinuity, then by a slow wave and, finally, by a slow combustion wave.

Some of these waves may be absent.

3. In order to distinguish the actually occurring evolutionary waves from the unrealizable nonevolutionary ones, we utilize the (v_{1X}, v_{2X}) plane in which the characteristic velocities U_-, U_X, U_+ are marked (cf. Fig. 1).

We first consider shock waves unaccompanied by a release of energy ($q = 0$). By utilizing the boundary conditions (7) — (12) ($\zeta = 0$) we can determine the Hugoniot line in the (v_{1X}, v_{2X}) plane. From the calculations of Bazer and Ericson[13,14] it follows that the values v_{1X} and v_{2X} lie on the line 1—2—3—4—5—6 in the case of slow waves, and on the line 7—8—9 for fast waves (cf. Fig. 1). The line 0—1—4—8—32 corresponds to the absence of a discontinuity $v_{1X} = v_{2X}$.

The segments 1—2—3—4 and 8—9 correspond to compressional shock waves $v_{1X} > v_{2X}$. In such waves the entropy is increasing.[14-15]

For $v_{1X} \to \infty$ the line 8—9 has the asymptote

$$v_{2x}^2 = (\gamma - 1)\,U_{2+}^2/2\gamma + (\gamma + 1)\,U_{2x}^2/2\gamma \qquad (U \ll c).$$

The segments 4—5—6—1 and 7—8 correspond to rarefaction shock waves $v_{1X} < v_{2X}$. In such waves the entropy is decreasing and, therefore, such waves cannot be realized.

The conditions for the shock waves to be evolutionary are of the following form[9,18-19]:

a) for the slow wave

$$U_{1-} < v_{1x} < U_{1x}, \qquad v_{2x} < U_{2-}; \tag{13}$$

b) for the fast wave

$$U_{1+} < v_{1x}, \qquad U_{2x} < v_{2x} < U_{2+} \tag{14}$$

The regions (13) and (14) are marked in Fig. 1 by vertical shading.

As can be seen from Fig. 1, the fast compression wave is an evolutionary wave along the whole segment 8—9, i.e., for arbitrary amplitudes. The slow compressional shock wave is evolutionary only along the segment 1—2. Along the segment 2—3—4 the slow compressional shock wave is a nonevolutionary one, and cannot be realized in spite of the fact that the entropy in such a wave is increasing.

We now consider discontinuities at which energy is released ($q > 0$). Such discontinuities are shown for $U \ll c$ and $q \ll c^2$ by the lines 0—10—11—12—4—13—14—15—4—16—17 and 18—19—20 in Fig. 1. Near the point $v_{1X} = U_{1-}$, $v_{2X} = U_{2-}$ these lines are described by the equation

$$(v_{1x} - U_{1-})^2 - (v_{2x} - U_{2-})^2 = \tfrac{3}{2}(\gamma - 1)\, q c_1^{-4} U_{1x}^2 U_{1y}^2, \tag{15}$$

near the point $v_{1X} = U_{1X}$, $v_{2X} = U_{2X}$ they are described by the equation

$$(v_{1x} - U_{1x})^2 - [1 - 2(\gamma - 1)\, q\, U_{1y}^{-2}]\,(v_{2x} - U_{2x})^2 = 0 \tag{16}$$

and, finally, near the point $v_{1X} = U_{1+}$, $v_{2X} = U_{2+}$ they are described by the equation

$$(v_{1x} - U_{1+})^2 - (v_{2x} - U_{2+})^2 = \tfrac{1}{2}(\gamma^2 - 1)\, q. \tag{17}$$

For $v_{1X} \ll U_{1-}$ this line is described by the equation

$$v_{2x} = [1 + (\gamma - 1)\, c_1^{-2} q]\, v_{1x}. \tag{18}$$

The segment 0—10 corresponds to slow combustion (rarefaction wave), the segment 15—4 corresponds to sub-Alfvén combustion (compression wave), the segment 4—16 corresponds to super-Alfvén combustion (rarefaction wave) and, finally, the segment 18—19 corresponds to fast combustion (compression wave). The segments 14—15 and 19—20 correspond to detonation in the case of slow and fast waves (compressional waves). Points 15 and 19 correspond to Chapman-Jouguet detonation in the case of slow and fast waves. The

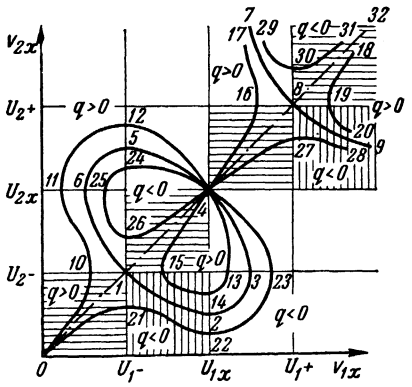

FIG. 1

segments 10—11—12—4—13—14 and 16—17 correspond to nonevolutionary discontinuities and, therefore, cannot be realized.

Figure 1 also shows discontinuities corresponding to absorption of energy ($q < 0$). Such discontinuities correspond to the lines 0—21—22—23—4—24—25—26—4—27—28 and 29—30—31. The segment 21—22 corresponds to ionization in the case of a slow shock wave, the segment 27—28 corresponds to ionization in the case of a fast shock wave.[4]

The boundary conditions (10)—(12) enable us to determine the change in the magnetic field in combustion waves.

From (10) and (11) it follows that

$$H_{2y} = \frac{1/\rho_1 - H_x^2/4\pi j^2}{1/\rho_2 - H_x^2/4\pi j^2} H_{1y} \tag{19}$$

($j = \rho_1 v_{1X} = \rho_2 v_{2X}$). From Eqs. (3)—(6) and (19) it follows that in all four magnetohydrodynamic combustion waves the transverse magnetic field H_y does not change sign. Taking into account the fact that both in slow and in super-Alfvén combustion the density is decreasing ($\rho_2 < \rho_1$), while in the case of sub-Alfvén and of fast combustion the density is increasing ($\rho_2 > \rho_1$), we obtain from (19) that in cases of slow and of fast combustion the transverse magnetic field H_y is increasing, while in cases of sub-Alfvén and super-Alfvén combustion the transverse magnetic field is decreasing.

4. We now go on to the question of the types of magnetohydrodynamic waves that can accompany a combustion wave. In order to simplify the problem we assume that the medium is bounded by a perfectly conducting piston moving with constant velocity **u**. Moreover, we assume that the piston velocity and the Alfvén velocity **U** are both much smaller than the velocity of sound c, and that the reaction energy q is much smaller than the square of the velocity of sound. We restrict ourselves to

the case in which the magnetic field, the piston velocity and the normal to the piston surface all lie in the same plane (the xy plane).

We first consider fast combustion. The conservation laws (7) — (12) enable us to express the discontinuities in the velocity, and the discontinuity in the specific volume, in terms of the velocity of propagation of the combustion front v_{1X} with respect to a stationary medium ($\zeta = 0$). The corresponding formulas can be greatly simplified in the limiting case $v_{1X} \gg c$:

$$\Delta_c v_x = (\gamma - 1)\, q/v_{1x}, \qquad \Delta_c v_y = -(\gamma - 1)\, U_x U_y q/v_{1x}^3,$$
$$\Delta_c V = -(\gamma - 1)\, qV/v_{1x}^2. \qquad (20)$$

As a result of electrodynamic viscosity[20] the relative velocity of the medium is equal to zero at the surface of the piston. Therefore, the sum of the discontinuities of the velocity for all the waves is equal to the velocity of the piston:

$$\Delta_c \mathbf{v} + \Delta_+ \mathbf{v} + \Delta_A \mathbf{v} + \Delta_- \mathbf{v} = \mathbf{u}, \qquad (21)$$

where $\Delta_c \mathbf{v}$ denotes the discontinuity in the velocity of the combustion wave. $\Delta_\pm$ is the discontinuity for the fast and the slow magnetohydrodynamic waves (without release or absorption of energy) and Δ_A is the amount of the Alfvén discontinuity. These discontinuities in the velocity are related to the discontinuity in the specific volume by means of the following relations:[4]

$$\Delta_+ v_x = -c\left(1 - \frac{\gamma+1}{4}\frac{\Delta_+ V}{V}\right)\frac{\Delta_+ V}{V},$$

$$\Delta_+ v_y = \frac{U_x U_y}{c}\left(1 - \frac{3-\gamma}{4}\frac{\Delta_+ V}{V}\right)\frac{\Delta_+ V}{V}; \qquad (22)$$

$$\Delta_- v_x = -U_x \frac{\Delta_- V}{V}, \qquad \Delta_- v_y = -\frac{c^2}{U_y}\frac{\Delta_- V}{V}; \qquad (23)$$

$$\Delta_A v_x = 0, \qquad \Delta_A v_y = 2U_y. \qquad (24)$$

Formulas (23) are valid only if the additional restriction $|\Delta_- V/V| \ll U_y^2/c^2$ is imposed.

By taking the components of expression (21) along the x and y axes, and by expressing $\Delta_\pm \mathbf{v}$ in terms of $\Delta_+ V$ and $\Delta_- V$, we obtain a system of two equations in two unknowns: $\Delta_+ V$ and $\Delta_- V$. This system enables us to find the amplitudes of the fast and the slow magnetohydrodynamic waves, $\Delta_+ V$ and $\Delta_- V$. If $\Delta_\pm V < 0$ then the corresponding wave will be a shock wave, if $\Delta_\pm V > 0$, then the wave will be a self-similar one.

The possible types of magnetohydrodynamic waves accompanying a fast combustion wave are shown in Fig. 2a. In this diagram the longitudinal component of the velocity of the piston u_X has been plotted along the abscissa, and the transverse component u_Y has been plotted along the ordinate. (For the sake of definiteness we assume that the components H_X, H_Y of the magnetic field in the unperturbed medium are positive.) The letters C, S, R, A denote respectively the presence of the following waves: combustion, shock, rarefaction, and Alfvén discontinuity. The plus sign refers to the fast wave, the minus sign refers to the slow wave. The sequence in which the letters appear coincides with the sequence in which the waves follow each other.

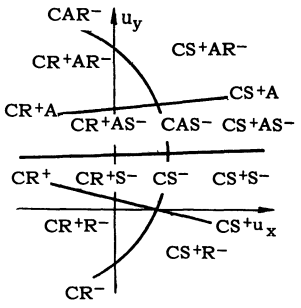

FIG. 2a

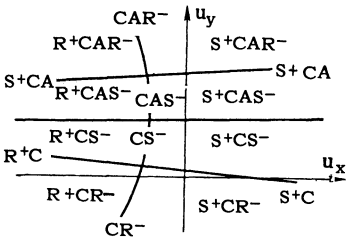

FIG. 2b

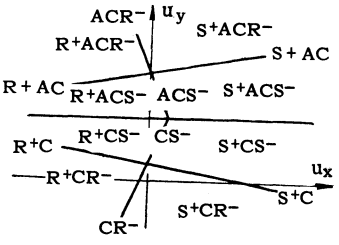

FIG. 2c

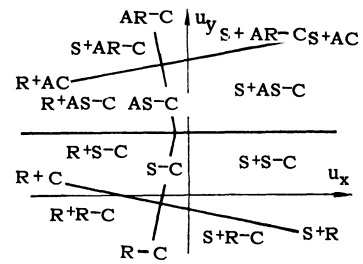

FIG. 2d

The origin in Fig. 2a lies in the region CR^+R^-. This means that in the case when the piston is at rest the fast combustion wave leads the others, it is followed first by the fast rarefaction wave and, finally, by the slow rarefaction wave. The same sequence of waves will also occur in the case when the piston is moving outward ($u_X < 0$, $u_Y = 0$). If the piston is moving inward ($u_X > 0$, $u_Y = 0$), then for sufficiently low velocity u_X we shall have the same combination of waves: CR^+R^-. As the piston velocity is increased the amplitudes of the fast and of the slow rarefaction waves diminish and, finally, vanish at the point where the horizontal axis intersects the lines CR^-, CS^-, CR^+, CS^+. (In the first approximation these lines intersect in one point.) As the piston velocity is increased further, we enter the region CS^+S^-.

In the case of transverse motion of the piston ($u_X = 0$) in the direction opposite to the direction of the transverse magnetic field in the unperturbed medium ($u_Y < 0$, $H_Y > 0$), with sufficiently low velocity $|u_Y|$ the same sequence of waves CS^+S^- occurs as in the case of the piston at rest. As the velocity $|u_Y|$ is increased the amplitude of the fast rarefaction waves diminishes and, finally,

vanishes on the line CR^-. This line separates the region CR^+R^- from the region CS^+R^- which is entered as the piston velocity $|u_y|$ is increased further.

In the case of the transverse motion of the piston ($u_x = 0$) in the direction of the magnetic field ($u_y > 0$, $H_y > 0$) with a sufficiently low velocity the same sequence of waves CR^+R^- occurs as in the case of the piston at rest. As the piston velocity is increased, the amplitude of the slow rarefaction wave diminishes and vanishes on the line CR^+. As the piston velocity u_y increases further a slow shock wave appears (regions CR^+S^-) whose amplitude increases with increasing piston velocity. Since in the case of the slow shock wave the transverse magnetic field H_y diminishes[17] (without changing sign), an increase in the transverse piston velocity u_y in the region CR^+S^- corresponds to a decrease in the transverse magnetic field H_y at the surface of the piston. When the piston velocity u_y becomes equal to

$$U_y - \frac{\gamma - 1}{2}\frac{U_y q}{c v_{1x}}$$

[cf. formula (28)], the transverse magnetic field H_y behind the slow shock wave (i.e., at the surface of the piston) vanishes.

As the piston velocity u_y increases further a sharp qualitative change in the flow pattern takes place. Behind the fast rarefaction wave R^+ an Alfvén wave A appears which changes the direction of the magnetic field by 180°, and the Alfvén wave is followed by a slow shock wave S^-. On the line separating the regions CR^+S^- and CR^+AS^- the amplitude of the slow shock wave reaches a maximum. As the piston velocity u_y increases the amplitude of the slow shock wave decreases, and this leads to an increase in the absolute value of the transverse magnetic field $|H_y|$ at the surface of the piston. In this case the transverse magnetic field at the surface of the piston is directed opposite to the transverse magnetic field in the unperturbed medium. Along the line CR^+A the amplitude of the slow shock wave vanishes, and as u_y increases further a slow rarefaction wave appears (region CR^+AR^-).

If we continue to increase the transverse piston velocity u_y, then the amplitude of the fast rarefaction wave diminishes, and vanishes along the line CAR^-. A further increase in the velocity of the piston u_y leads to the appearance of a fast shock wave (region CS^+AR^-). As can be seen from Fig. 2a, fast combustion is possible for any arbitrary piston velocity u.

The equations of the lines bounding the various regions in Fig. 2a are of the following form:

the lines CR^-, CS^-, CAS^-, CAR^-

$$u_x + \frac{U_x}{2c^2}(u_y - 2U_y)\,u_y - (\gamma - 1)\frac{q}{v_{1x}} = 0, \qquad (25)$$

the lines CR^+, CS^+

$$u_y + \frac{U_x U_y}{c^2}u_x - (\gamma - 1)\frac{U_x U_y q}{v_{1x}c^2} = 0, \qquad (26)$$

the lines CR^+A, CS^+A

$$u_y - 2U_y - \frac{U_y}{c}u_x + (\gamma - 1)\frac{U_y q}{v_{1x}c} = 0. \qquad (27)$$

The line separating the regions CR^+S^- and CR^+AS^-, and also the line between the regions CS^+S^- and CS^+AS^-, is determined by the equation

$$u_y - U_y - \frac{1}{2}\frac{U_y}{c}u_x + \frac{\gamma - 1}{2}\frac{U_y q}{v_{1x}c} = 0. \qquad (28)$$

5. We now proceed to consider super-Alfvén combustion. The discontinuities in the velocity and in the specific volume in a super-Alfvén combustion wave are determined in the limiting case $U_{1X} \ll v_{1X} \ll U_{1+}$ by the relations

$$\Delta_c v_x = -(\gamma - 1)\,q v_{1x}/c^2, \qquad \Delta_c v_y = (\gamma - 1)\,U_x U_y q / v_{1x}c^2;$$
$$\Delta_c V = (\gamma - 1)\,qV/c^2. \qquad (29)$$

The possible types of magnetohydrodynamic waves accompanying a super-Alfvén combustion wave are shown in Fig. 2b.

The equations of the lines bounding the various regions of Fig. 2b are of the following form:

the lines CR^-, CS^-, CAS^-, CAR^-

$$u_x + \frac{U_x}{2c^2}(u_y - 2U_y)\,u_y + (\gamma - 1)\frac{q v_{1x}}{c^2} = 0, \qquad (30)$$

the lines R^+C, S^+C

$$u_y + \frac{U_x U_y}{c^2}u_x - (\gamma - 1)\frac{U_x U_y q}{v_{1x}c^2} = 0, \qquad (31)$$

the lines R^+CA, S^+CA

$$u_y - 2U_y - \frac{U_y}{c}u_x + (\gamma - 1)\frac{U_y}{c^2}q = 0. \qquad (32)$$

The line separating the regions R^+CS^- and R^+CAS^-, and also the line separating the regions S^+CS^- and S^+CAS^- are determined by the equation

$$u_y - U_y - \frac{1}{2}\frac{U_y}{c}u_x + \frac{\gamma - 1}{2}\frac{U_y q}{c^2} = 0. \qquad (33)$$

As can be seen from Fig. 2b, super-Alfvén combustion is possible for any arbitrary piston velocity u.

6. We now consider sub-Alfvén combustion in the limiting case $U_X - v_{1X} \ll U_X$. The discontinuities in the velocity and in the specific volume in the sub-Alfvén combustion wave are determined by the relation

$$\Delta_c v_x = 2(\gamma - 1)\frac{U_x - v_{1x}}{U_y^2} q, \qquad \Delta_c v_y = (\gamma - 1)\frac{q}{U_y},$$

$$\Delta_c V = -2(\gamma - 1)\frac{U_x - v_{1x}}{U_x U_y^2} qV. \tag{34}$$

The possible types of magnetohydrodynamic waves accompanying a sub-Alfvén combustion wave are shown in Fig. 2c. The equations of the lines bounding the various regions in Fig. 2c have the following form:

the lines CR^-, CS^-

$$u_x - \frac{U_x U_y}{c^2} u_y + (\gamma - 1)\frac{U_x}{c^2} q = 0, \tag{35}$$

the lines ACS^-, ACR^-

$$u_x + \frac{U_x U_y}{c^2}(u_y - 2U_y) + (\gamma - 1)\frac{U_x}{c^2} q = 0, \tag{36}$$

the lines R^+C, S^+C

$$u_y + \frac{U_x U_y}{c^2} u_x - (\gamma - 1)\frac{q}{U_y} = 0, \tag{37}$$

the lines R^+AC, S^+AC

$$u_y - 2U_y - \frac{U_y}{c} u_x + (\gamma - 1)\frac{q}{U_y} = 0. \tag{38}$$

As can be seen from Fig. 2c, sub-Alfvén combustion is possible for any arbitrary piston velocity u.

7. Finally, we consider slow combustion in the limiting case $v_{1x} \ll U_x$. The discontinuities in the velocity and in the specific volume in the slow combustion wave are determined by the relations

$$\Delta_c v_x = -(\gamma - 1) q v_{1x}/c^2,$$

$$\Delta_c v_y = -(\gamma - 1) U_y q v_{1x}/c^2 U_x,$$

$$\Delta_c V = (\gamma - 1) qV/c^2. \tag{39}$$

The possible types of magnetohydrodynamic waves accompanying the slow combustion wave are shown in Fig. 2d.

The equations of the lines bounding the various regions in Fig. 2d have the following form:

the lines R^-C, S^-C

$$u_x - \frac{U_x U_y}{c^2} u_y + (\gamma - 1)\frac{q v_{1x}}{c^2} = 0, \tag{40}$$

the lines AS^-C, AR^-C,

$$u_x + \frac{U_x U_y}{c^2}(u_y - 2U_y) + (\gamma - 1)\frac{q v_{1x}}{c^2} = 0, \tag{41}$$

the lines R^+C, S^+C

$$u_y + \frac{U_x U_y}{c^2} u_x + (\gamma - 1)\frac{U_y q v_{1x}}{c^2 U_x} = 0, \tag{42}$$

the lines R^+AC, S^+AC

$$u_y - 2U_y - \frac{U_y}{c} u_x - (\gamma - 1)\frac{U_y q v_{1x}}{c^2 U_x} = 0. \tag{43}$$

As can be seen from Fig. 2d, slow combustion is possible for any arbitrary piston velocity u.

The authors express their gratitude to A. I. Akhiezer for valuable discussions.

[1] É. Larish and I. Shekhtman, JETP **35**, 203 (1958), Soviet Phys. JETP 8, 139 (1959).

[2] Gross, Chinitz, and Rivlin, J. Aero Space Sci. **27**, 283 (1960).

[3] G. A. Lyubimov, Dokl. Akad. Nauk SSSR **126**, 532 (1959), Soviet Phys. Doklady **4**, 526 (1960).

[4] V. P. Demutskii and R. V. Polovin, J. Tech. Phys. (U.S.S.R.) **31**, 419 (1961), Soviet Phys. Tech. Phys. **6**, 302 (1961).

[5] Ya. B. Zel'dovich and A. S. Kompaneets, Теория детонации (The Theory of Detonation), Gostekhizdat, 1955, p. 112.

[6] S. R. Pottasch, Revs. Modern Phys. **30**, 1053 (1958).

[7] F. D. Kahn, ibid. **30**, 1058 (1958).

[8] A. Goldsworthy, ibid. **30**, 1062 (1958).

[9] Akhiezer, Lyubarskii, and Polovin, JETP **35**, 731 (1958), Soviet Phys. JETP **8**, 507 (1959).

[10] I. M. Gel'fand, Usp. Mat. Nauk **14**, 87 (1959).

[11] R. V. Polovin, Usp. Fiz. Nauk **72**, 33 (1960), Soviet Phys. Uspekhi **3**, 677 (1961).

[12] L. D. Landau and E. M. Lifshitz, Механика сплошных сред (Mechanics of Continuous Media), Gostekhizdat, 1953.

[13] J. Bazer and W. B. Ericson, Astrophys. J. **129**, 758 (1959).

[14] W. B. Ericson and J. Bazer, Phys. Fluids **3**, 631 (1960).

[15] S. V. Iordanskii, Dokl. Akad. Nauk SSSR **121**, 610 (1958), Soviet Phys. Doklady **3**, 736 (1959).

[16] R. V. Polovin and G. Ya. Lyubarskii, JETP **35**, 510 (1958), Soviet Phys. JETP **8**, 351 (1959).

[17] R. V. Polovin and G. Ya. Lyubarskii, Ukr. Phys. J. **3**, 571 (1958).

[18] V. M. Kontorovich, JETP **35**, 1216 (1958), Soviet Phys. JETP **8**, 851 (1959).

[19] S. I. Syrovat-skii, JETP **35**, 1466 (1958), Soviet Phys. JETP **8**, 1024 (1959).

[20] G. Ya. Lyubarskii and R. V. Polovin, Dokl. Akad. Nauk SSSR **128**, 684 (1959), Soviet Phys. Doklady **4**, 977 (1960).

Translated by G. Volkoff
298